Pacific Northwest
NATIONAL LABORATORY
Proudly Operated by Battelle Since 1965

Tel: (509) 375-7331
Fax: (509) 375-7340
MSIN: P7-03
mark.murphy@pnnl.gov

June 2, 2015

Dr. Oren M. Milstein
StemRad, Ltd.
6 Raoul Wallenburg St. 3rd Floor
Ramat Hachayal
Tel Aviv, 6971905, Israel

Dear StemRad LTD :

SUBJECT: FINAL TEST REPORT FOR STEMRAD'S *360 GAMMA*™ PERSONAL PROTECTION DEVICE – PNWD Project Number 66845

Attached is the final report describing the test protocols and data results involving the testing of the StemRad *360 Gamma*™ *Personal Protection Device* on PNNL's anthropomorphic male phantom with real human skeleton (Alderson RANDO® model), using TLD chips within phantom cavities to measure the internal dose from a Cs-137 source both with and without the *360 Gamma*™ device on phantom.

Please contact us for any questions on this report. It was a pleasure working with your staff and being able to assist your company with product characterization. We hope you consider us for assistance with any future testing.

Sincerely,

Mark K. Murphy
Sr. Research Scientist
Radiation Measurements & Irradiations

<MKM/MKM/mkm>

Enclosure/Attachment

PACIFIC NORTHWEST NATIONAL LABORATORY
operated by
BATTELLE
for the
UNITED STATES DEPARTMENT OF ENERGY
under Contract DE-AC05-76RL01830

Test Report - StemRad® 360 Gamma™ Radiation Shielding Device

Report Date	June 2, 2015
Project Title	Testing of the StemRad® 360 Gamma™ Personal Protection Device
PNNL Project Manager	Mark K. Murphy, Radiation Measurements & Irradiations Group
PNNL Project/Proposal Number	66845
Customer:	StemRad LTD
Customer Point of Contact	**Dr. Oren M. Milstein – StemRad LTD** **oren@stemrad.com** **U.S. Office:** **228 Hamilton Ave. Palo Alto, CA 94301** **650-388-9112 (Tel) 650-388-9120 (Fax)**

BACKGROUND

StemRad LTD is a private company based in Tel Aviv, Israel, with offices in Palo Alto, CA. StemRad LTD developed a product called the StemRad® 360 Gamma™, which is a "personal **protection** device" that is worn like a belt, and **that wraps around the hips in order to shield the bones that conta**in a significant percentage of the body's bone marrow. The obj**ective is to conserve enough viable bone marrow from an otherwise deadly radiation dose to allow regeneration of bone marrow and survival of the individual.**

StemRad LTD staff Dr. Oren M. Milstein (CSO) and Daniel Levitt (CEO), and their U.S. consultant Dr. Kenneth Kase, visited staff from the Radiation Measurements & Irradiations Group at Pacific Northwest National Laboratory (PNNL) on May 9, 2014, to see the irradiation and dosimetry processing labs and to discuss details of the desired TLD measurements within phantom wearing the StemRad® 360 Gamma™ device. Discussions during that visit, and numerous email communications afterwards, resulted in the final protocols used.

CUSTOMER REQUIREMENTS AND EXPECTATIONS

StemRad's desire was for **PNNL to perform irradiations of the RANDO® male phantom that would result in an approximate simulation of a radiation exposure of an individual to** a "cloud" of C**esium-137 (Cs-137) radioactivity, while still being consistent with the irradiation geometry of previous phantom irradiations conducted by StemRad in Israel. This source-phantom irradiation geometry could also simulate the radiation dose to an individual walking and turning numerous times in an enclosed environment that contains multiple sources at various heights relative to the individual. After discussions between StemRad and PNNL staff, StemRad selected the source-phantom geometry options listed in Table 1.**

Table 1. RANDO® and Cs-137 Source Irradiation Geometry Selected By StemRad for Subject Testing

RANDO Height * Off Floor	Source Movement#	Number of Source Positions and Angles	Dwell Times at Each Angle	Dose to RANDO Reference Point* at Each Source Position	RANDO-Source Distance at 0° †
170 cm	**Vertical in straight line**	**-**45°, **-22.5**°, 0°, +22.5°, +45 °	**Equal**	**Varying (due to varying source distance)**	**130 cm**

*** Measured relative to the reference point, located on the top surface of slice 29.**

 # The maximum source height possible with existing equipment is 304 cm.

† This distance, combined with RANDO® height and straight line source movement, results in lowest position of source being ~40 cm off floor (and thus ~4.5% floor scatter at that position) and highest position being 300 cm off floor.

StemRad also desired that the irradiations be done with TLDs located in tissue and bone within the hip and abdominal areas, including within bone marrow in the hip bones and vertebrae and within the GI tract. Of course, irradiations would be performed for the two cases of StemRad® 360 Gamma™ device ON and OFF.

PROJECT OBJECTIVES

The project objective is to provide data that shows the effectiveness (decrease in dose to hip and abdominal area) of the StemRad® 360 Gamma™ device for the approximate simulation of a "cloud" of Cs**-137 radioactivity.**

TEST EQUIPMENT

The equipment utilized during this project are listed in Table 2. PNNL's **male RANDO® phantom, manufactured by Alderson Corp., was used for the irradiations. The RANDO® man represents a 175** cm (5'9") tall and 73.5 **kg (162 lb.) male figure. It does not have arms or legs. The phantom is constructed with a real human skeleton which is cast inside soft tissue-simulating material. Lungs are molded to fit the contours of the natural rib cage. The air space of the head, neck and stem bronchi are duplicated. The phantom is sliced at 2.54-cm intervals to allow access to various parts and, in particular, to the cavities for radiation detectors. Each slice contains approximately 40 of these cavities, each 4.8 mm diameter in a 3.5 cm grid pattern.**

The Cs-137 source used has a current activity of 4.85 Ci, and is contained within three layers of encapsulation consisting of a total of 0.078" stainless steel and 0.125" aluminum. This

Table 2. Equipment Utilized for StemRad® 360 Gamma™ Belt Irradiations on Phantom

Equipment Model	Serial Number	Use	Calib Expiration Date
StemRad® 360 Gamma™ belt, Small-Tall size	SR360019	Allow measurement of effectiveness of belt in Cs-137 field	N/A
Alderson RANDO® anthropomorphic phantom, with real skeleton	N/A	Allow measurement of effectiveness of belt in reducing radiation dose rate to specific regions of a human	N/A
4.85 Ci Cs-137 Source, triple encapsulation	318-030	Irradiations of RANDO® phantom with and without belt	02/2016
Capintec Model PR-18 ionization chamber	5889	Both calibration and real-time monitoring of radiation field	04/2016
Keithley Model 617 electrometer	383823	Collect signal from ionization chamber	06/2015
Temperature probe	TNFL1-0001	Temperature and pressure values allow corrections to ionization signal due to air density	02/2016
Barometric pressure	PEEW1-0001		02/2016
Timer	SWCC1-0001	Provide accurate durations of radiation exposure for each position and total duration.	02/2016
Harshaw TLD-700 Lithium-fluoride Thermoluminescent Dosimeters (TLD) chips(0.32mm x 0.32 mm x 0.9 mm)	StemRad set	Placed within RANDO® cavities, allows measurement of total integrated radiation dose	Calib 4/2015
Harshaw Model 5500 TLD Reader	WD33697	Allows automated readout and analysis of TLDs	N/A
Automated turntable at 1 rpm, attached to the top of aluminum frame on a hydraulic cart	N/A	Allows continuous rotation of RANDO phantom	N/A

results in the elimination of the beta particle part of the spectrum associated with the unencapsulated nuclide, and only the gamma spectrum is seen (peaks at 662 keV).

PREPARATION FOR TESTING

Even though the RANDO® phantom already contained approximately 40 cavities in each slice, StemRad desired dose information at additional locations, especially in bone. In order to determine the exact locations for these additional cavities, StemRad used ImageJ software

to construct 3D models of the red bone marrow within the RANDO® phantom. The 2D images of each slice face (provided by PNNL) were loaded into the segmentation editor of ImageJ as image stacks and the red bone marrow regions were highlighted as regions of interest and interpolated to form 3D volumes of the red bone marrow within the RANDO® slices. Because of the relative spatial uniformity of the spinal column, the vertebral volumes were assigned one TLD cavity only for each slice (totaling 7 cavities). The remaining 33 cavity locations were then identified by calculating the center of masses of 33 equal volumes of the pelvic red bone marrow within these slices. This StemRad-developed method allows StemRad to match absorbed doses in these cavities to specific masses of red bone marrow within the lower spine and pelvis. At StemRad's direction, PNNL drilled 40 additional cavities at the identified locations, in 11 of the slices that involved the hip and abdominal area (slices 22-32). Two images of each of these 11 slices are provided in Appendix A: one image with StemRad's labeled locations for desired TLD locations, and another image showing PNNL's labeled cavities into which TLDs were inserted for the RANDO® irradiations – for a total of 22 images. StemRad determined that the 40 TLD cavity locations which required drilling into bone are representative of red bone marrow tissue and the other 52 TLD cavity locations are representative of other tissues in the abdominal region. Refer to Appendix C to discern the tissue associated with each measurement location.

Another modification to the RANDO® phantom was to mill down "high spots" at the interfaces of about six of the phantom slices. This was needed in order to make the assembled phantom much more stable, and ensure that the slices in the spinning phantom would not shift during the 8-10 hour irradiation.

In order to provide secure attachment of RANDO® to the turntable, and still maintain natural thigh shape, mass, and radiation scatter; thigh extensions were fabricated from tissue-equivalent polymer and were attached to the turntable, and allowed attachment to RANDO® thighs using polymer dowels. The turntable was secured to the very edge of a hydraulic cart that could raise RANDO® from approximately 60 cm to 200 cm in height.

Because source-to-RANDO and floor-to-RANDO distances were important, as were the irradiation angles, it was required to have a RANDO reference point. StemRad selected a point near the middle of the RANDO® torso, located on the top surface of slice #29 and at the geometric center of that slice, which is at the point of an existing TLD cavity (see slice #29 image in Appendix A). To ensure that the z-axis of RANDO® rotated exactly relative to this selected reference point on slice #29, first the polymer thigh extensions were placed on a level surface, then RANDO® slices were stacked on top of the polymer thigh extensions until slice #29 was complete (and using carpenter's level, ensuring slice surfaces stayed level). A carpenter's plumb-bob – suspended from above – was lowered to slice #29 and centered on the reference point. Then the top slice was removed, the plumb-bob lowered and rotation axis location on this next slice labeled, and this repeated until axis of rotation on slices 29-34 and the polymer thigh extension were all labeled. This marked axis of

rotation on the polymer thigh extension allowed it to be aligned on turntable exactly as desired to allow RANDO® to rotate relative to the slice #29 reference point. When RANDO was stacked all the way to his neck, the plumb-bob was again used to mark the point of rotation on the top of each slice (slices 10-30), and it was observed that this axis of rotation consistently stayed aligned with the same central cavity/plug on each slice.

In order to provide a secure anchor at the top of the spinning RANDO®, a ¾-inch piece of plywood with a 7/8-inch hole in the center was screwed to the top of RANDO® (the slice representing the base of the neck), and a 7/8-inch wood dowel (secured by an overhead arm) was inserted into the hole. The overhead arm is constructed of hollow, thin-walled aluminum frame, which resulted in less than 0.4% scatter of radiation field in direction of RANDO® (this was measured by placing the aluminum frame next to a Model RO-20 radiation survey meter in the Well Room Cs-137 field).

In order to allow movement of the Cs-137 source vertically during RANDO® irradiations, a thin-walled PVC pipe (cut in half to form a half-pipe) was used to hold the source, and this source holder was raised to a maximum height of 300 cm by being attached to a Genie Lift. The Genie Lift is a strong, low mass fork lift that was manually operated from 300 cm using a long rod (allowing operator to stay outside high radiation fields).

The "fit" or **exact positioning of the 360 Gamma™ belt on the RANDO® phantom to** StemRad's desired specifications was accomplished **by PNNL staff placing the belt on RANDO®, taking digital photos from numerous angles, emailing the photos to StemRad staff,** and adjusting the belt based on feedback from StemRad. This process took over a week's **time because the medium-sized belt was found to be slightly too large for RANDO®, and so StemRad shipped their small-sized belt. Based on the photos provided to StemRad (see Figure 1), the small-sized belt provided an acceptable fit according to StemRad. This acceptable fit was defined as the back of the belt spanning between slice 24.5 and slice 33.5, and the front of the belt spanning between slice 25.3 and slice 32.3, which resulted in the midpoint of belt span on both front and back being well within 0.5 cm of the desired reference point of slice 29.0 (top of slice 29).**

The RANDO® cavities the TLDs would occupy were cleaned with alcohol to ensure no luminescent debris would get on TLD chips, then these cavities were labeled with marked masking tape to ensure accurate TLD placement and documentation.

Figure 1. Photos of small-sized belt on RANDO® phantom. These photos allowed StemRad staff to verify that the fit met with their specifications.

TEST PROTOCOL USED

The TLD and phantom preparation, source-phantom geometry, and irradiation protocol was as follows:

- **TLD-700 LiF TLDs were used, and analyzed with a Harshaw Model 5500 reader. Before each use/irradiation, the TLDs were reader annealed using a linear time-temperature profile (TTP) with a heating rate of 10°C/s, starting at 50°C and reaching a maximum temperature of 300°C, for a total heating time of 43 seconds. The reader anneal was followed by a low temperature oven anneal at 80°C for 24 hours to reduce the abundance of short half-life traps in the TLD crystal and thus reduce fading of signal.**
- **Within two days prior to RANDO® irradiations, at one slice at a time the TLDs were loaded into desired RANDO® cavities (3 TLDs per cavity) at the center height within the phantom slice, and the resulting voids at the top and bottom of the cavities were filled with unit density plugs. The total number of test cavities involved was 92, resulting in 276 TLD test chips, which did not count the TLD chips used for controls and calibration set. TLD location is documented as to slice#, cavity#, wheel#, and wheel position# (there were 7 separate wheels or circular cartridges used for automated readout of TLDs, with 50 slots in each wheel to accommodate 50 TLD chips).**
- **An additional cavity at shoulder level of RANDO® (slice 13) was loaded with TLDs for both irradiations. This was in order to allow comparison of total integrated dose for belt ON and belt OFF scenarios and make any corrections if necessary. The cavity used was only approximately 1 cm depth in tissue, and mid-way between shoulders, and would not be impacted by presence or absence of StemRad belt.**
- **In addition, 50 reader calibration chips, 12 QC chips, 12 blank chips and 40 spares were used to support the measurement process.**
- **The phantom slices were then stacked on top of turntable to complete the phantom assembly, and well secured with long strips of industrial adhesive tape. Then top anchor was put in place.**
- **The RANDO®/Turntable/Cart assembly was then rolled into the Low Scatter Facility and placed at desired location near center of the room. The room is approximately 8 x 9 x 10 meters in size.**
- **The Monitoring Chamber was then centered at RANDO® reference height (top of slice 29) and at 14.5 cm from RANDO® surface (right side of RANDO®) and secured. This chamber would provide gamma field intensity monitoring in real-time, and allow immediate verification at each of the 5 source positions that source radiation field was at correct intensity relative to RANDO®. This would provide backup data for the passive monitoring (TLDs in cavity in slice 13). It should be noted here that the measured tissue dose from chips in slice 13 is not expected to match the tissue dose inferred from the air kerma measured by the monitoring chamber due to the shielding provided by the phantom during rotation.**
- **RANDO/cart was then raised until top of slice 29 was at predetermined irradiation height of 170 cm.**

- **Source holder (without source) was raised to each of the 5 positions, and both source height and RANDO-Source distances were measured and verified (See Table 3 for resulting angles and distances).**
- **Video monitoring was then turned on, as well as turntable at 1 rpm.**
- **The source holder was set at the first irradiation position (-45 degrees = 40 cm height) and, using a 180 cm handling tool, the source was quickly transferred from its storage container to the source holder. The stopwatch was started when source was within the PVC holder, and the PVC lid flipped into position. Photos in Figures 2a and 2b provide view of actual setup just prior to irradiation #2.**
- **After the preselected irradiation duration had elapsed (1 hour 36 minutes), using a 3.5 meter rod outside the high radiation area, the Cs-137 source is quickly cranked vertically to the next highest position. This movement is accomplished within about 15-20 seconds.**
- **After each predetermined irradiation duration (1 hour 36 minutes) the source is moved to next irradiation position for a total of 5 positions listed in Table 3.**
- **As the irradiation is completed at the last source position (highest position, + 45 degrees and 300 cm height), the source is quickly lowered to the lowest position (~25 seconds) and then transferred back to its shielded storage container away from RANDO® (~ 10 seconds).**
- **The phantom/cart is then lowered and rolled back to the dosimetry lab.**
- **At some time prior to TLD analysis, RANDO® is dismantled one slice at a time and** TLDs removed from its cavities. The TLDs are placed into "wheels" (Trays used in **automated reader), and TLD location is documented as to slice#, cavity#, wheel #, and wheel position#.**
- **At the predetermined TLD post irradiation fade time (~ 2-4 days), the loaded TLD reader wheels were placed in the TLD Reader for readout and analysis.**
- **Reader Calibration was accomplished by reading chips exposed under CPE conditions behind 6.9 mm of PMMA plastic in a chip irradiation jig mounted on a 30 cm x 30 cm x 15 cm PMMA phantom. The chips were exposed with their front face located at a distance of 3 meters from the source, using a J.L Shepherd Cs-137 beam irradiator to achieve a delivered air kerma corresponding to D(10) = 10 mGy, based on C_K = 1.21 (ANSI/HPS N13.11-2009). The calibration chips were annealed, exposed and read at the same time as the test chips exposed in phantom.**
- **The entire process was repeated for the second RANDO® irradiation.**
- **The TLD results were then populated into a spreadsheet and resulting dose levels calculated. The data results included providing the ratio of the mean dose from each RANDO® cavity for both belt ON/OFF scenarios in order to provide a measure of belt effectiveness to Cs-137 field.**

Table 3. Angles, distances and exposure rates associated with RANDO and Cs-137 source.

Source Position	Source Height Off Floor (cm)	Source-Slice 29 Reference Distance (cm)	Source-RANDO Z-axis Distance (cm)	mR/h in AIR (slice 29)	mR in 1.6 hrs in AIR (slice 29)
+45˚	300	184	130	379	606
+22.5˚	224	141	130	645	1032
0˚	170	130	130	759	1214
-22.5˚	116	141	130	645	1032
-45˚	40 (~4.5% scatter)	184	130	396	634
* Air-Kerma, Gy, is obtained by multiplying Exposure, R, by 8.78E-3				Total Exposure: 4.518 R *Total Air-Kerma: 3.967 cGy	

Figure 2a. Photo of wide view of actual setup just prior to irradiation Run #2, with RANDO (belt ON) on left, and white PVC source holder on bottom right.

Figure 2b. Photos of actual setup just prior to irradiation Run #2, showing sample Cs-137 source (polished aluminum) in its white PVC holder, RANDO rotating with belt ON, and monitoring chamber.

DATA RESULTS

A copy of the irradiation datasheet, showing the verified angles, distances, irradiation durations, and monitoring chamber signal is provided in Appendix B. For any given run, the real-time monitoring chamber data indicated that the signals for the paired angles (±22.5 ° and ±45 °) were within 1.5% of each other when the known ~4.5 % scatter at **-**45 ° **position is accounted for. Comparing the monitoring chamber signals for run#1 and run#2 shows the dose rates for the two runs were within 1.5% of each other. This is consistent with the TLD results from slice 13, which indicate the total doses for run#1 and run#2 were within about 1%. This agreement, along with verifying the distances before each run, provides assurance that for run#1 and run#2 RANDO® experienced the same irradiation angles, distances, dose rates, and total delivered dose.**

Appendix C contains the spreadsheet that includes the average measured absorbed dose in tissue for each TLD cavity, for both Belt Off and Belt On conditions. Also included are the ratios of absorbed dose for Belt On and Belt Off conditions for these tissue types, as well as the associated standard deviations of the data. Table 4 summarizes these measured absorbed dose values for the various tissue types. Table 5 summarizes the Belt On/Belt Off dose ratio for each of the regions or tissue types.

The symmetry in the X-Y plane for doses measured within RANDO® without the shielding belt, as indicated by the values in the spreadsheet in Appendix C, is due to a combination of

Table 4. Summary of measured absorbed dose in tissue by body region or tissue type, for both Belt OFF and Belt ON conditions.

Body Region/Tissue Type	Absorbed Dose – Belt OFF		Absorbed Dose – Belt ON	
	Mean *	%SDEV †	Mean *	%SDEV #
Bone Marrow - Hip	2797 mrad	3.0	1637 mrad	15.4
Bone Marrow - Vert	2770 mrad	3.8	1922 mrad	17.7
Bone Marrow – Hip & Vert	2792 mrad	3.2	1687 mrad	17.0
GI Tract	2818 mrad	3.2	2081 mrad	10.4
Ovaries**	2693 mrad	0.5	1765 mrad	0.1
Combined	2.80 rad (2.80 cGy)	3.2	1.90 rad (1.90 cGy)	16.5

*** Dose values are the integrated absorbed dose relative to tissue.**

† In addition to the high accuracy and precision of the TLDs, these tight standard deviations are due to a combination of symmetric source-RANDO geometry, the fact RANDO was irradiated from all sides, the relatively large distance of the source approximated a point-source geometry and minimal variation in "in**-**air" dose rate across RANDO volume, and th**e penetrating ability of Cs-137 gamma spectrum in tissue.**

 # The reason these standard deviations are as good as they are, is due to the same combination of reasons above; but deviation is greater because the fact that not all the TLD locations were shielded fully by the shielding belt for the entire exposure.

**** These would be the approximate ovary locations if this RANDO was female based on anatomical markers.**

Table 5. Summary of the Belt ON/Belt OFF dose ratio for each of the regions or tissue types.

Body Region/ Tissue Type	Min Ratio	Max Ratio	Belt ON/Belt OFF Dose Ratio	
			Mean	%SDEV
Bone Marrow - Hip	0.42	0.76	0.59	17.0
Bone Marrow - Vert	0.49	0.87	0.70	19.4
Bone Marrow – Hip & Vert	0.42	0.87	0.61	18.6
GI Tract	0.62	0.87	0.74	9.8
Ovaries	0.652	0.659	0.656	0.7
Combined	0.42	0.87	0.68	16.5

the following:

- **The symmetry of the physical RANDO® (tissue and bone) in the X-Y dimension.**
- **The symmetry of the effective density of RANDO in the X-Y dimension.**
- **The symmetry in the X-Y dimension of the cavities containing TLDs.**
- **The source distance, and thus dose rate, being equal for each pair of same-symmetry TLD cavities.**
- **RANDO® completing numerous rotations at a constant speed during exposure.**
- **The fact that the axis of rotation for RANDO® was very near the geometric center of each slice, especially the slices containing TLDs.**

Measurements of the Cs-137 radiation field at 170 cm height and distances of 120 cm and 130 cm were also performed without RANDO® in place in order to provide the exposure rate and air-kerma rate "free**-in-**air". The measured **exposure rates of 759 mR/h (0.666 cGy/h Air-kerma rate) at the 130 cm reference distance, and the 889 mR/h (0.781 cGy/h Air-kerma rate) at 120 cm indicates, as expected, that the field follows $1/d^2$. This will allow in-air dose rates to be calculated for any location in free space, so any location where RANDO® volume could reside. This would be useful to compare in-air dose rate versus tissue or bone dose rate (and therefore total integrated dose) at any point for a stationary RANDO® phantom.**

MEASUREMENT UNCERTAINTIES

The radiation measurement uncertainties that PNNL's Radiation Measurements & **Irradiations group calculate for their operations, using GUM Workbench software, are consistent with NIST Technical Note 1297 (1994), as well as a document produced by Working Gr**oup 1 of the Joint Committee for Guides in Metrology in 2008 titled "**Evaluation of Measurement Data -** Guide to the Expression of Uncertainty in Measurement". The **measurement uncertainty values that were expected to be of most interest to StemRad were those that involved the MEASURED AIR-KERMA RATE (and integrated AIR-KERMA) at the location where RANDO would be placed, the resulting MEASURED ABSORBED DOSE to RANDO TISSUES, and the BELT ON/BELT OFF MEASURED DOSE RATIOS for these same**

tissue regions.

Uncertainty in the Measured Air-Kerma: Because StemRad may desire to use the testing results to create factors that convert from a known Exposure rate (R/time) or Air-Kerma rate (Gy/time) of a field, to the dose within RANDO (wearing the StemRad belt) placed in such a field (for example, Absorbed Dose in specified organs or Effective Dose Equivalent), the measurement uncertainties associated with these Exposure and Air-Kerma parameters (See Table 3) would be helpful. The expanded uncertainty associated with these Exposure and Air-Kerma values were calculated to be ± 1.15% at the 67% confidence level (k = 1), and ± 2.3% at the 95% confidence level (k=2).

Uncertainty in TLD Measured Dose: As can be expected, the main uncertainty components involve the precision of the readout values of the TLD chips. Given that the TLD system was calibrated prior to RANDO® irradiation using one of PNNL's calibrated Cs**-137 fields, the uncertainties in the resulting Gy and Gy/hr values measured within RANDO® are not influenced by the source-RANDO geometry (distances and angles). As can be seen on the spreadsheet in Appendix C, which details the TLD measurement results for the various regions or tissue types, for the Belt Off irradiation the standard deviation of the measured absorbed dose varied between 0.5% and 3.8%, with the standard deviation for all tissues combined being 3.2% (See Table 4). Propagating all uncertainties, the total expanded uncertainty for the quoted ABSORBED DOSES within the RANDO® cavities at the specified locations with Belt Off was calculated to be ± 2.4% at the 67% confidence level (k = 1), and ± 4.8% at the 95% confidence level (k = 2).**

For the Belt On irradiation, the standard deviation in the measured absorbed dose varied between 0.1% and 17.7%, with the standard deviation for all tissues combined being 16.5% (See Table 4). Propagating all uncertainties , the total expanded uncertainty for the quoted ABSORBED DOSES within the RANDO® cavities at the specified locations with Belt On was calculated to be ± 3.1% at the 67% confidence level (k = 1), and ± 6.2% at the 95% confidence level (k = 2).

For the Belt On/Belt Off dose ratios, the standard deviation varied between 0.7% and 19.4%, with the standard deviation for all tissues combined being 16.5% (See Table 5). Propagating all uncertainties, the total expanded uncertainty for the Belt On/Belt Off dose ratios for cavities at the specified locations was calculated to be ± 4.0% at the 67% confidence level (k = 1), and ± 7.9% at the 95% confidence level (k = 2).

The details in the various components of uncertainty and how they were propagated to arrive at the expanded uncertainty values above are provided in Appendix D. In addition to using the TLD chip readout accuracy and precision values described above (the main contribution to error), the overall expanded uncertainty takes into account other variables such as the physical measurement of the source-RANDO distances at the various angles, estimated Cs-137 source anisotropy, and the results of the quality control dosimetry in phantom slice 13.

The individual raw TLD readout values will be provided separately from this report, as well as additional photos and video of spinning phantom in irradiation setup.

Report written by:

Mark K. Murphy, Sr. Research Scientist — 6/3/2015 Date

Report reviewed by:

Bruce Rathbone, Sr. Research Scientist — 6/3/2015 Date

APPENDIX A - StemRad's provided photos (left) showing their desired X-Y coordinates for TLD cavities, and PNNL's provided photos (right) showing resulting TLD cavities. RANDO® phantom slices 22-32.

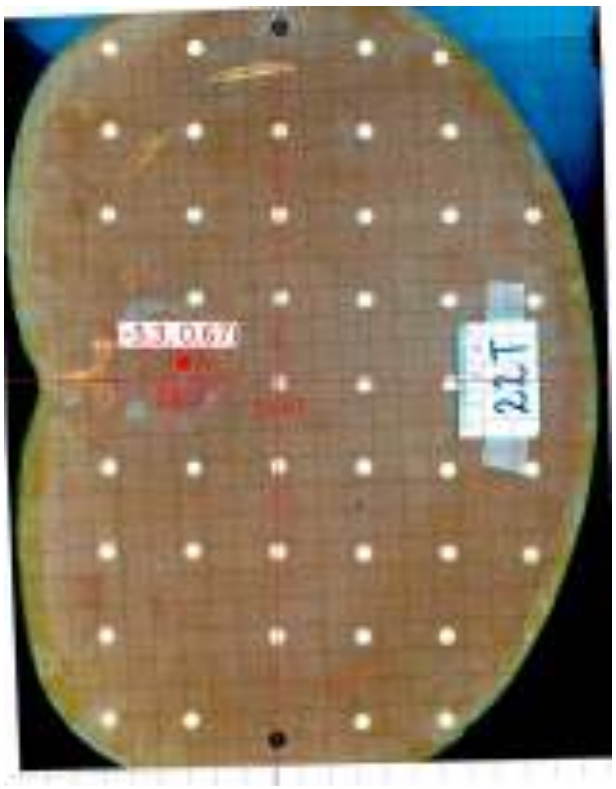

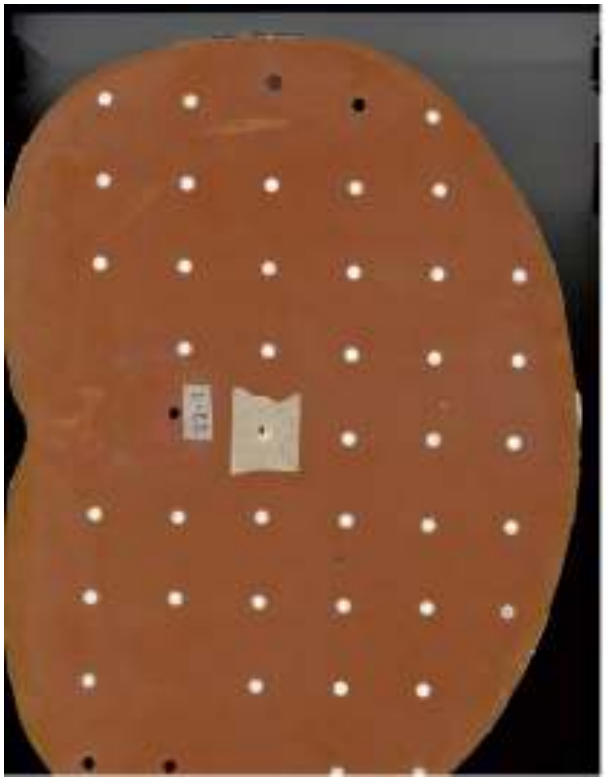

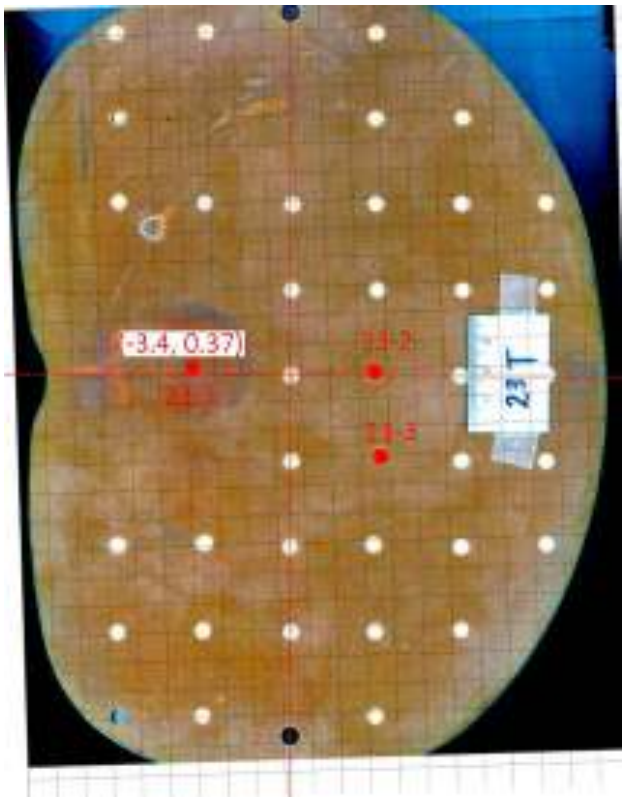

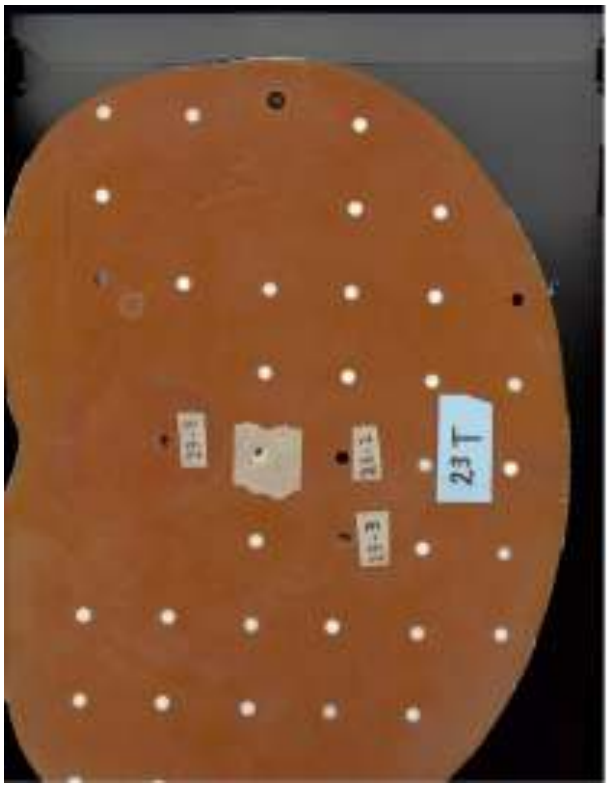

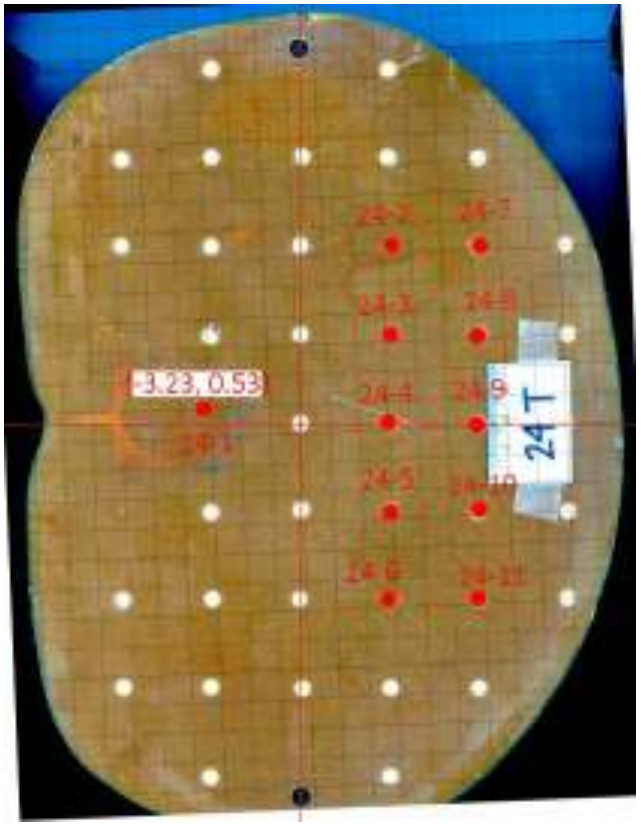
-3.23, 0.53
24 T

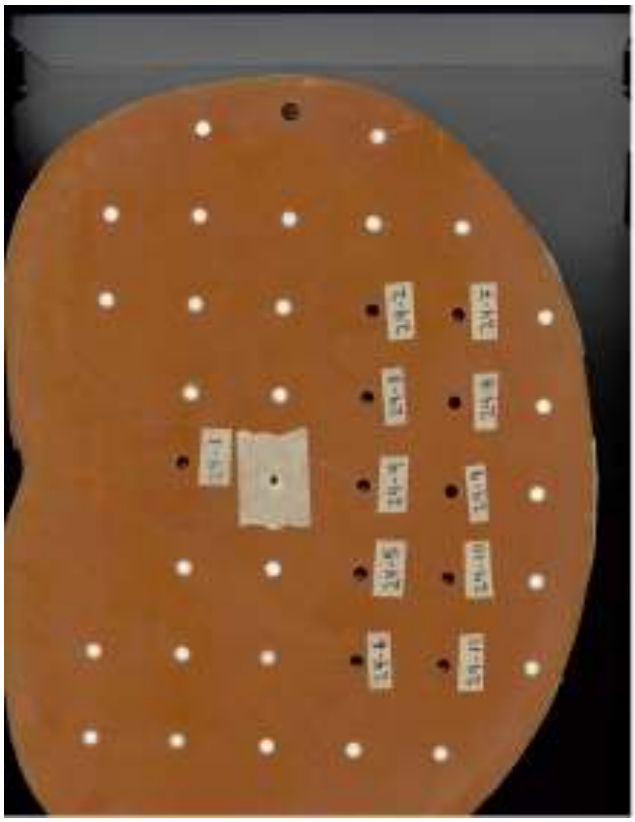

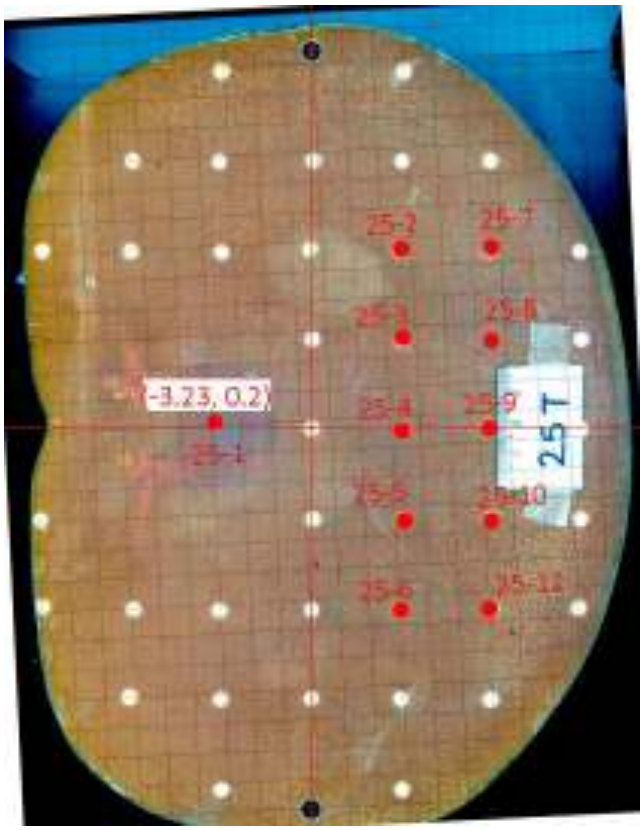
-3.23, 0.2
25 T

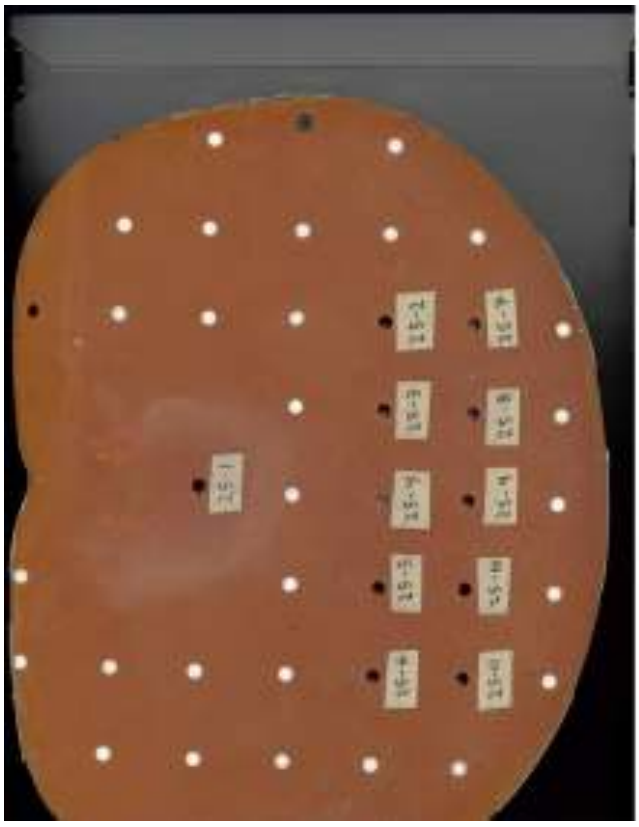

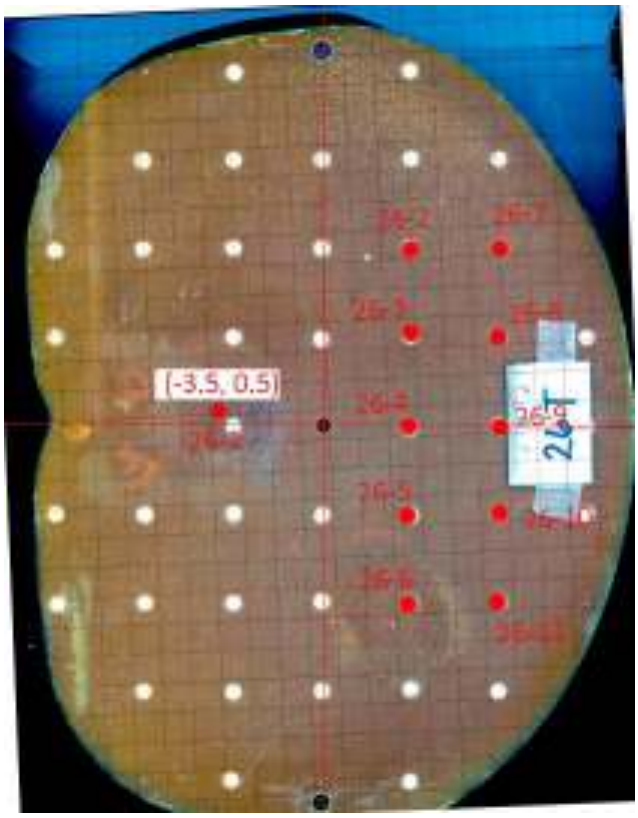
(-3.5, 0.5)
26T

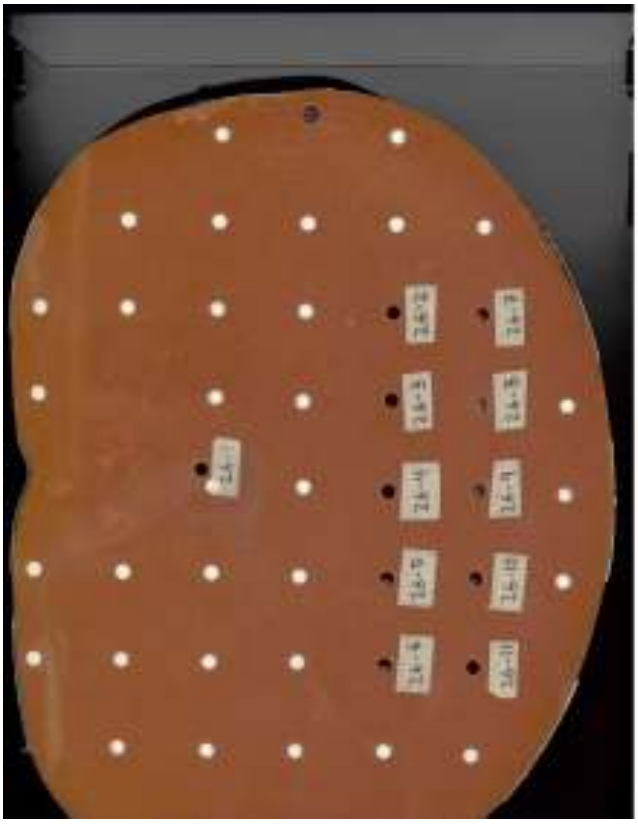

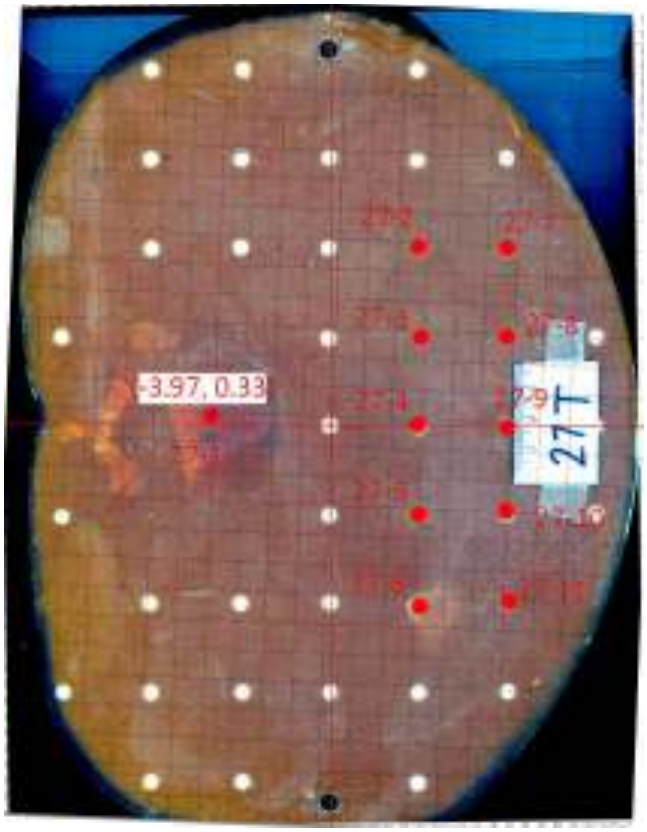
-3.97, 0.33
27T

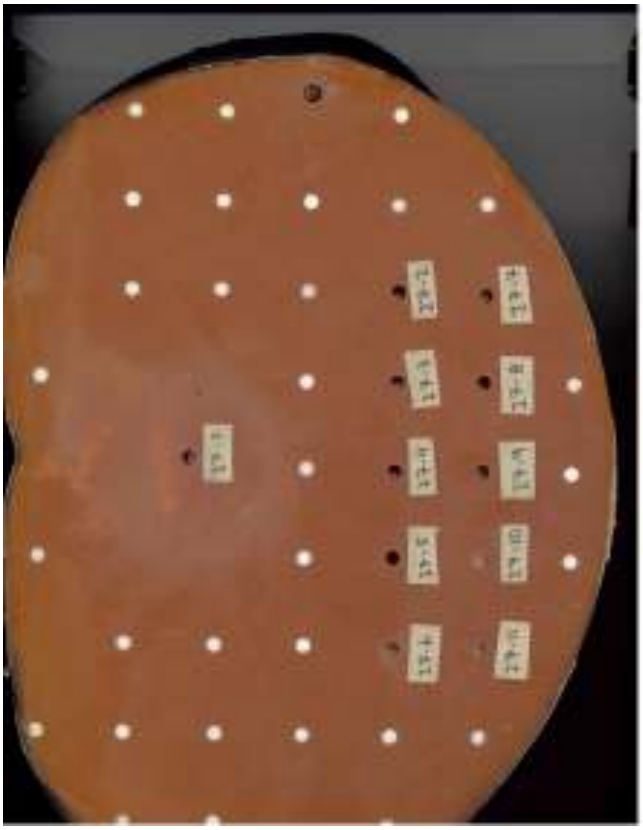

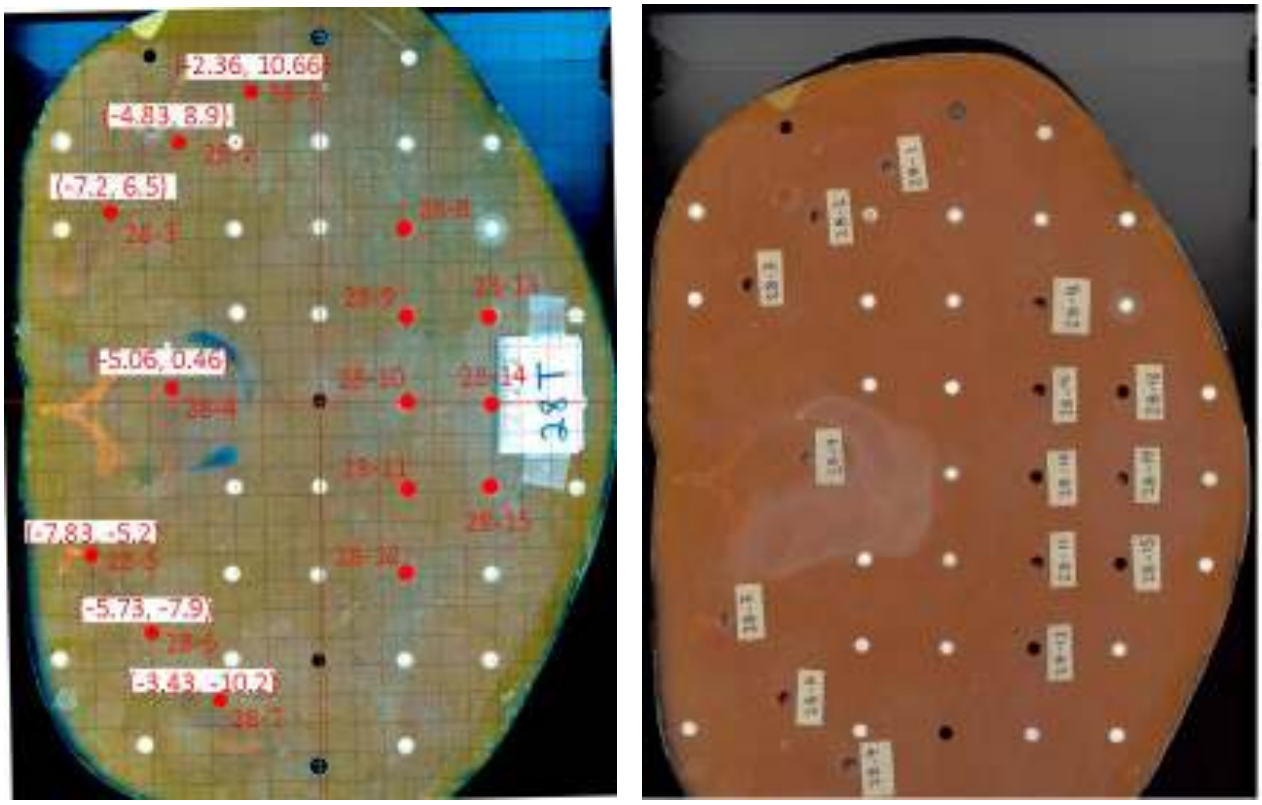
-2.36, 10.66
-4.83, 8.9
-7.2, 6.5
-5.06, 0.46
28 T
-7.83, -5.2
-5.73, -7.9
-3.43, -10.2

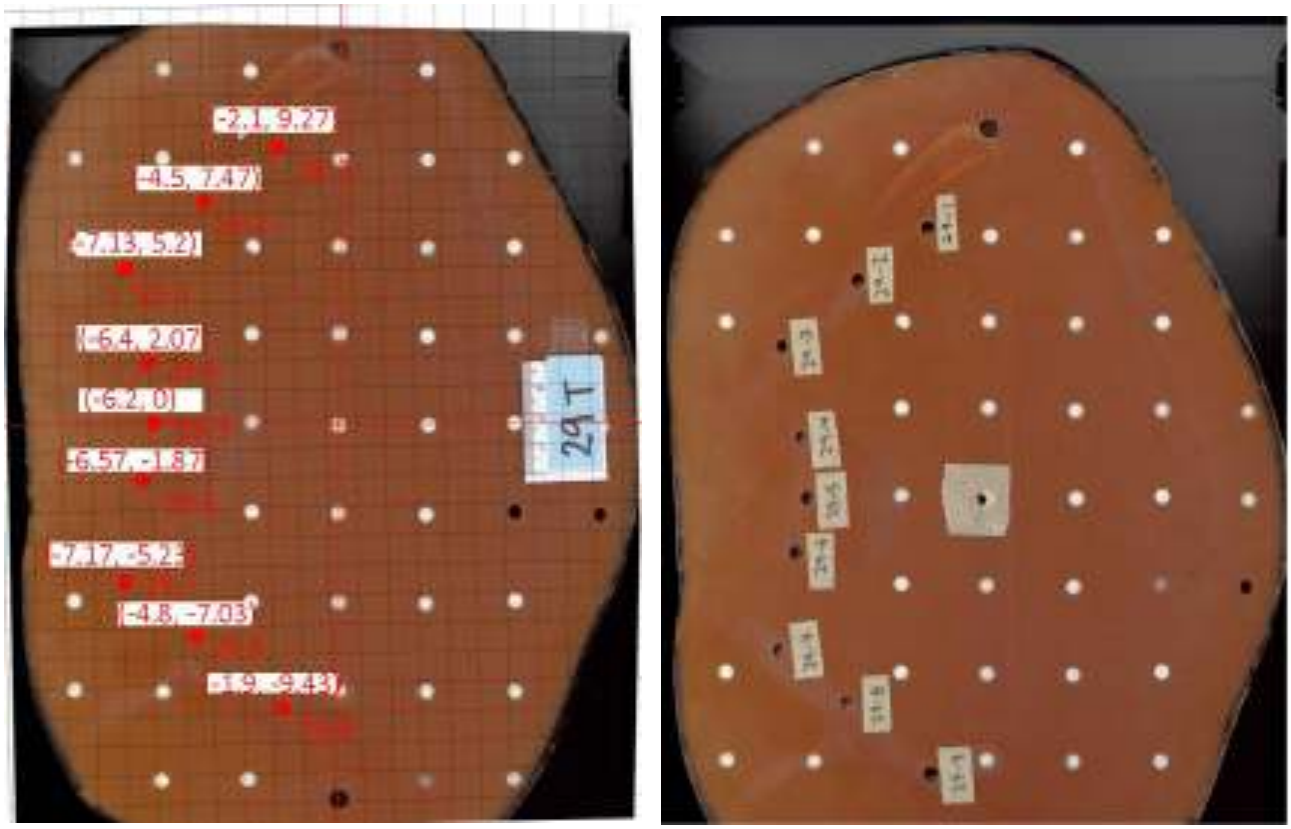
-2.1, 9.27
-4.5, 7.47
-6.4, 2.07
-6.57, -1.87
-7.17, -5.2
-4.8, -7.03
29 T

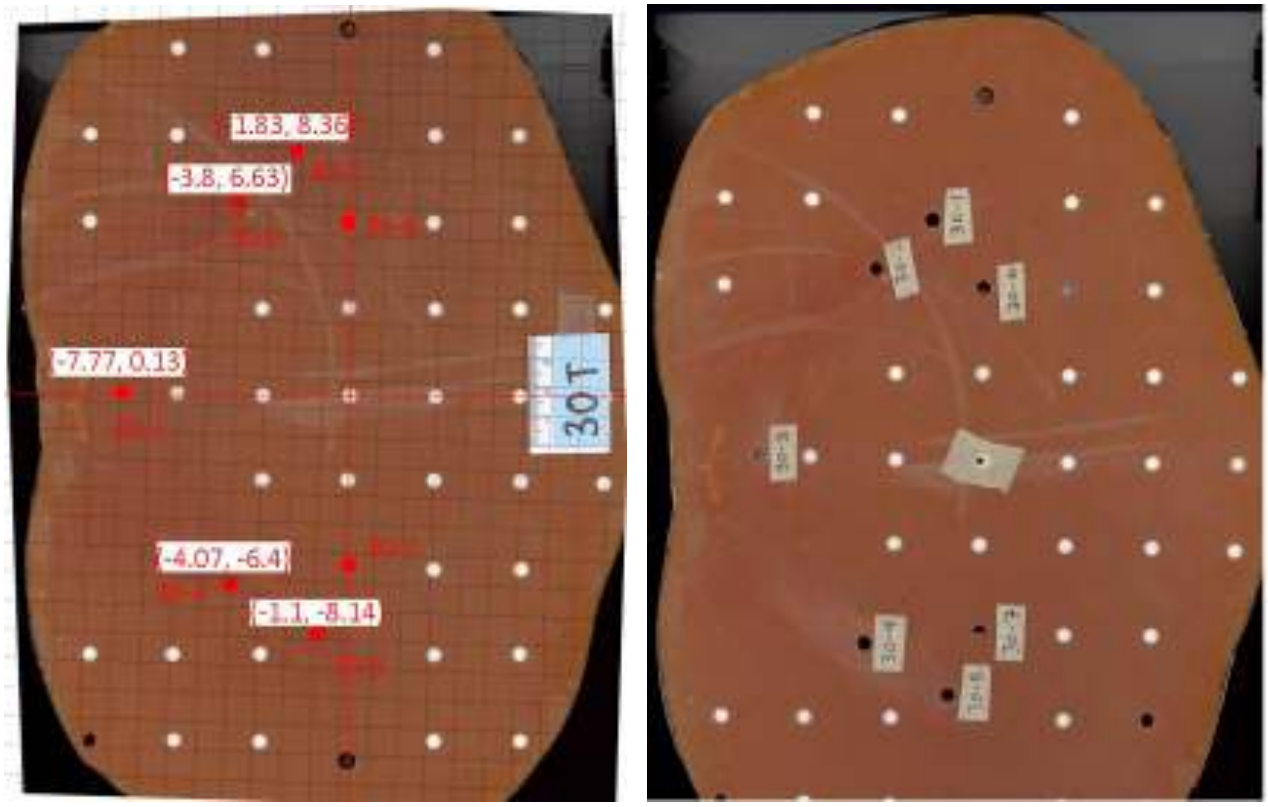
1.83, 8.36
-3.8, 6.63
-7.77, 0.13
30 T
-4.07, -6.4
-1.1, -8.14

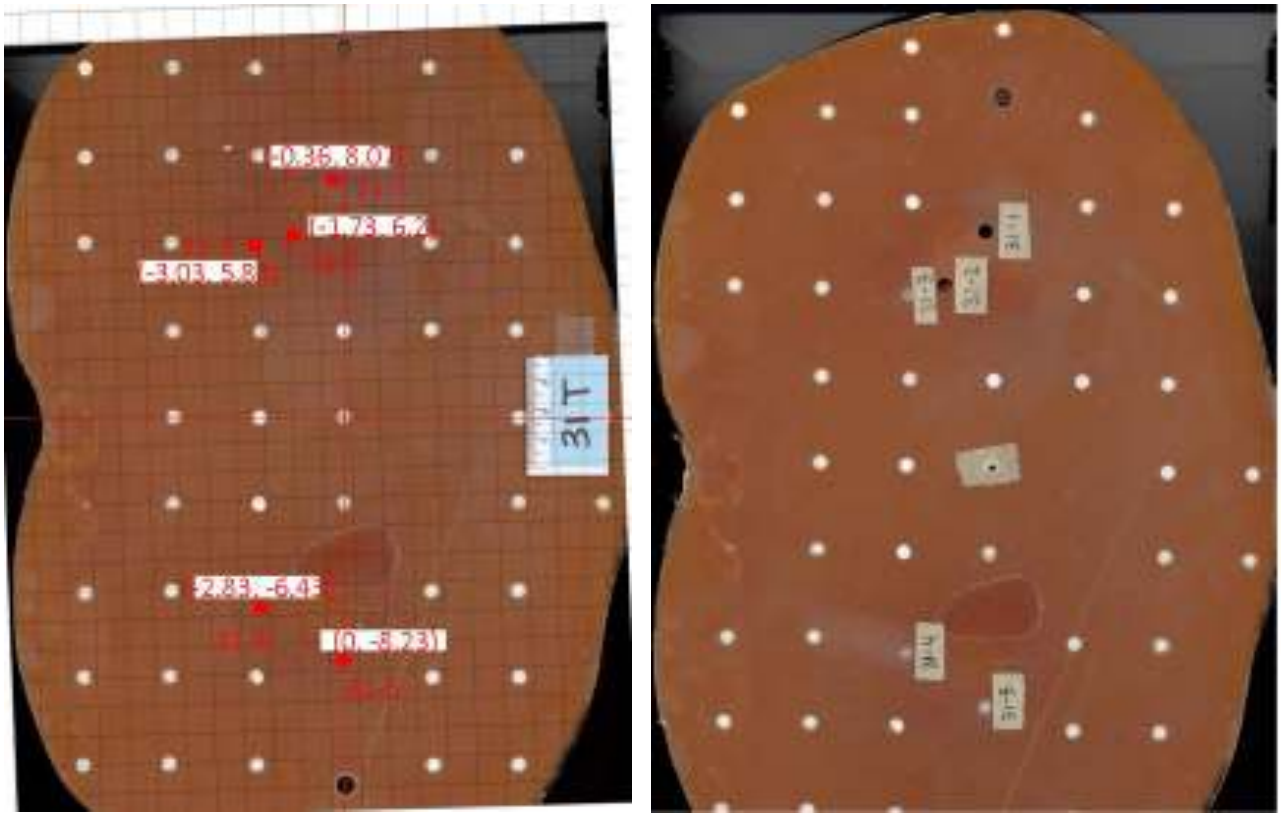
31 T

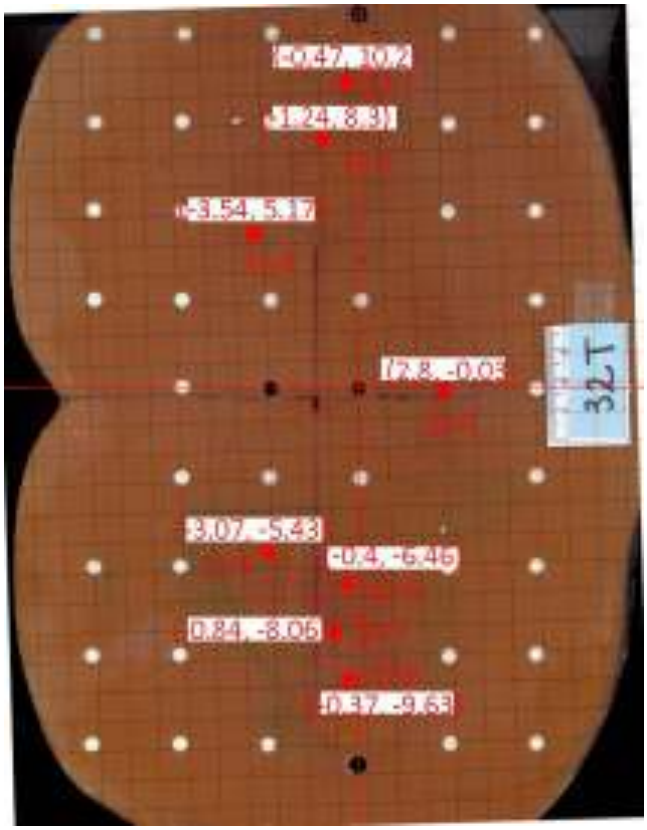
32T

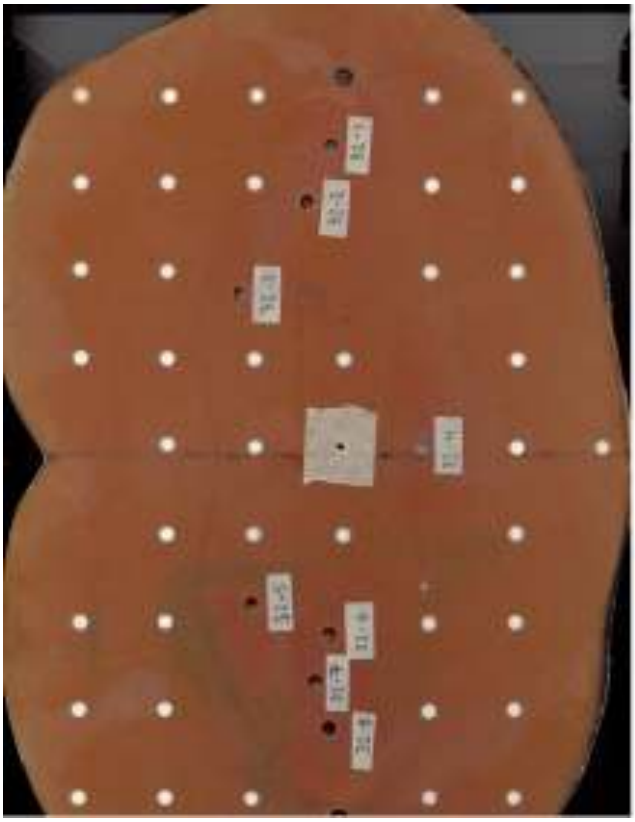

StemRad Shielding Belt Testing Using RANDO Phantom and TLDs

Run #1: 4-1-2015 (TLD Load Date) | MK Murphy A. Maine (TLDs Loaded By) | 4-2-2015 (Irradiation Date) | MK Murphy (Irradiation Performed By) | 47.0" = 119.4 cm (Source/RANDO Surface Dist at 0°)

4-6-2015 (TLD Unload Date) | J. Pirkkanen (TLDs Unloaded By) | 4/7/2015 (TLD Readout Date) | AL Maine (TLD Readout By)

Belt ON/OFF? ☑ RANDO spinning at 1 rpm ☑ RANDO Slice 29T at 170 cm off floor ☑ PR-18/RANDO Dist = 5.75 "

Source Position	Angle *	Source Distance Off Floor	Source* /RANDO Distance	Irrad Start Time	Irrad Duration	Source Transit Time	Temp & Press	Monitoring Chamber Readings (pA)	Comments
1	-45°	40 cm ✓	184 cm ✓	6:55A	1h36m	~5 sec	22.1 C 759 mm	-59.5 -59.3 -59.6 -59.5	source move t=0
2	-22.5°	116 cm ✓	141 cm ✓	8:31A	1h36m	~20 sec	22.0 760	-92.3 -92.6 -92.4 -92.6	t=1h36m ✓
3	0.0°	170 cm ✓	130 cm ✓	10:07	1h36m	~20 sec	22.2 760	-104.6 -104.9 -104.4 -104.5	t=3h12m ✓
4	+22.5°	224 cm ✓	141 cm ✓	11:43	1h36m	~20 sec	22.3 760	-90.7 -90.8 -90.6 -91.0 -91.3 -91.2	t=4h48m ✓
5	+45°	300 cm ✓	184 cm ✓	1:21	1h36m	~25 sec	21.6 760	-57.0 -56.7 -56.1 -56.9 -57.3 -57.4	t=6h24m ✓
* Measured relative to reference point at top of slice #29									t=8h0m ✓ off

Run #2: 4-14-2015 (TLD Load Date) | J. Pirkkanen (TLDs Loaded By) | 4-17-2015 (Irradiation Date) | MK Murphy J. Pirkkanen (Irradiation Performed By) | 47.0" = 119.4 cm (Source/RANDO Surface Dist at 0°)

4-20-2015 5 PM (TLD Unload Date) | J. Pirkkanen (TLDs Unloaded By) | 4-21-2015 @ 0830 (TLD Readout Date) | AL Maine (TLD Readout By)

Belt ON/OFF? ☑ RANDO spinning at 1 rpm ☑ RANDO Slice 29T at 170 cm off floor ☑ PR-18/RANDO Dist = 5.75 "

↳ Front of belt spans from slice 25.3 to 32.3, and back of belt spans from slice 24.5 to 33.5

Source Position	Angle *	Source Distance Off Floor	Source* /RANDO Distance	Irrad Start Time	Irrad Duration	Source Transit Time	Temp & Press	Monitoring Chamber Readings (pA)	Comments
1	-45°	40 cm ✓	184 cm ✓	7:38A	1h36m	~5 sec	21.3 C 759.2 mm	-58.9 -58.7 -58.5 -58.6	source Move t=0 ✓
2	-22.5°	116 cm ✓	141 cm ✓	9:14A	1h36m	~20 sec	21.4 C 759.2 mm	-90.9 -91.2 -91.3 -91.1	t=1h36m ✓
3	0.0°	170 cm ✓	130 cm ✓	10:50A	1h36m	~20 sec	21.9 C 758.4 mm	-103.2 -103.1 -102.6 -102.7	t=3h12m ✓
4	+22.5°	224 cm ✓	141 cm ✓	12:27P	1h36m	~15 sec	21.9 756	-89.7 -89.9 -90.04 -90.2 -89.7 -90.07	t=4h48m ✓
5	+45°	300 cm ✓	184 cm ✓	2:02P	1h36m	~15 sec	22.8 755	-55.9 -56.0 -55.8 -56.0 -56.1	t=6h24m ✓
* Measured relative to reference point at top of slice #29						~25 sec	end -55.7 -55.9 -56.0 -55.8		t=8h0m ✓ off

MiTE on back page

~15 sec before source taken off holder

Appendix C

TLD Data Results for TLDs Contained Within RANDO Phantom - StemRad Belt

Measurement Location			Belt Off			Belt On			Belt On / Belt Off		
Phantom Slice Number	Slice Cavity Number	Tissue Type	Absorbed Dose (mrad)	Relative Standard Uncertainty	Relative Expanded Uncertainty k=2	Absorbed Dose (mrad)	Relative Standard Uncertainty	Relative Expanded Uncertainty k=2	Ratio	Relative Standard Uncertainty	Relative Expanded Uncertainty k=2
23	2	BM (h)	2648	0.0121	0.0242	1442	0.0080	0.0159	0.490	0.0145	0.0290
23	3	BM (h)	2589	0.0189	0.0379	1533	0.0168	0.0376	0.447	0.0267	0.0534
23	4	BM (h)	2722	0.0078	0.0156	1478	0.0345	0.0683	0.542	0.0349	0.0696
23	5	BM (h)	2915	0.0149	0.0296	1236	0.0105	0.0210	0.424	0.0181	0.0363
23	6	BM (h)	2889	0.0107	0.0214	1360	0.0085	0.0170	0.474	0.0136	0.0273
23	7	BM (h)	2909	0.0201	0.0400	1488	0.0085	0.0170	0.512	0.0216	0.0439
29	1	BM (h)	2915	0.0157	0.0314	1567	0.0148	0.0298	0.534	0.0216	0.0433
29	2	BM (h)	2891	0.0083	0.0167	1487	0.0104	0.0209	0.531	0.0134	0.0267
29	3	BM (h)	2853	0.0087	0.0174	1370	0.0117	0.0234	0.480	0.0146	0.0292
29	4	BM (h)	2797	0.0080	0.0160	1401	0.0108	0.0212	0.506	0.0133	0.0266
29	5	BM (h)	2737	0.0086	0.0173	1417	0.0077	0.0154	0.518	0.0116	0.0232
29	6	BM (h)	2787	0.0120	0.0241	1350	0.0174	0.0348	0.490	0.0212	0.0433
29	7	BM (h)	2910	0.0104	0.0208	1363	0.0081	0.0162	0.466	0.0132	0.0283
29	8	BM (h)	2901	0.0137	0.0274	1470	0.0088	0.0188	0.525	0.0165	0.0338
29	9	BM (h)	2783	0.0082	0.0165	1507	0.0064	0.0168	0.540	0.0116	0.0239
30	1	BM (h)	2787	0.0115	0.0229	1537	0.0086	0.0172	0.551	0.0143	0.0287
30	2	BM (h)	2780	0.0084	0.0169	1578	0.0108	0.0217	0.568	0.0139	0.0275
30	3	BM (h)	2853	0.0141	0.0282	1437	0.0152	0.0304	0.500	0.0205	0.0415
30	4	BM (h)	2894	0.0132	0.0264	1548	0.0119	0.0239	0.575	0.0215	0.0430
30	5	BM (h)	2770	0.0104	0.0207	1595	0.0077	0.0154	0.612	0.0129	0.0258
31	1	BM (h)	2777	0.0083	0.0166	1634	0.0158	0.0317	0.660	0.0179	0.0358
31	2	BM (h)	2736	0.0089	0.0177	1745	0.0103	0.0206	0.638	0.0136	0.0271
31	3	BM (h)	2818	0.0102	0.0204	1806	0.0106	0.0212	0.641	0.0147	0.0294
31	4	BM (h)	2723	0.0082	0.0164	1740	0.0082	0.0165	0.639	0.0124	0.0247
31	5	BM (h)	2773	0.0103	0.0206	1837	0.0116	0.0233	0.663	0.0155	0.0311
32	1	BM (h)	2914	0.0083	0.0166	2130	0.0083	0.0165	0.730	0.0124	0.0248
32	2	BM (h)	2765	0.0100	0.0201	1998	0.0100	0.0200	0.725	0.0161	0.0321
32	3	BM (h)	2716	0.0162	0.0324	1901	0.0104	0.0208	0.700	0.0192	0.0385
32	4	BM (h)	2704	0.0081	0.0162	2043	0.0103	0.0206	0.755	0.0131	0.0263
32	5	BM (h)	2637	0.0094	0.0187	1883	0.0098	0.0196	0.709	0.0136	0.0271
32	6	BM (h)	2642	0.0082	0.0164	1940	0.0094	0.0188	0.731	0.0125	0.0250
32	7	BM (h)	2727	0.0083	0.0170	1978	0.0168	0.0338	0.725	0.0191	0.0382
32	8	BM (h)	2731	0.0090	0.0180	2034	0.0105	0.0210	0.729	0.0139	0.0277
	BM (h)	min	2637	0.0078	0.0156	1236	0.0077	0.0154	0.42	0.0116	0.0232
	BM (h)	max	2989	0.0251	0.0402	2130	0.0345	0.0683	0.78	0.0349	0.0696
	BM (h)	average	2797	0.0109	0.0219	average	1637	0.0120	0.59	0.0166	0.0331
	BM (h)	stdev	85	0.0032	0.0065	stdev	253	0.0051	0.10	0.0050	0.0099
	BM (h)	%stdev	3.0			%stdev	15.4		17.6		
22	1	BM (v)	2722	0.0081	0.0162	2380	0.0063	0.0186	0.874	0.0125	0.0247
22	1	BM (v)	2732	0.0079	0.0158	2187	0.0088	0.0177	0.804	0.0116	0.0237
24	1	BM (v)	2722	0.0141	0.0280	2148	0.0144	0.0289	0.788	0.0202	0.0404
25	1	BM (v)	2784	0.0165	0.0370	1949	0.0196	0.0393	0.699	0.0270	0.0540
26	1	BM (v)	2729	0.0159	0.0211	1743	0.0078	0.0183	0.638	0.0130	0.0260
27	1	BM (v)	2692	0.0102	0.0204	1662	0.0076	0.0153	0.560	0.0127	0.0255
28	1	BM (v)	2995	0.0101	0.0201	1479	0.0124	0.0249	0.494	0.0160	0.0320
	BM (v)	min	2692	0.0079	0.0158	1479	0.0076	0.0153	0.48	0.0116	0.0237
	BM (v)	max	2999	0.0165	0.0370	2380	0.0196	0.0393	0.87	0.0270	0.0540
	BM (v)	average	2770	0.0109	0.0211	1922	0.0117	0.0234	0.70	0.0156	0.0315
	BM (v)	stdev	106	0.0030	0.0073	340	0.0045	0.0090	0.14	0.0056	0.0112
	BM (v)	%stdev	3.8			17.7			19.4		
	BM (h & v)	min	2637	0.0078	0.0156	1236	0.0076	0.0153	0.42	0.0116	0.0232
	BM (h & v)	max	2999	0.0251	0.0402	2380	0.0345	0.0683	0.87	0.0349	0.0696
	BM (h & v)	average	2792	0.0110	0.0221	1687	0.0118	0.0237	0.61	0.0165	0.0330
	BM (h & v)	stdev	83	0.0033	0.0065	307	0.0049	0.0099	0.11	0.0060	0.0120
	BM (h & v)	%stdev	3.0			17.9			18.8		
23	2	GI	2711	0.0095	0.0188	2337	0.0098	0.0191	0.851	0.0134	0.0269
23	3	GI	2750	0.0117	0.0234	2371	0.0144	0.0287	0.862	0.0186	0.0370
24	2	GI	2786	0.0079	0.0159	2333	0.0082	0.0164	0.834	0.0114	0.0228
24	3	GI	2732	0.0093	0.0186	2280	0.0062	0.0164	0.827	0.0124	0.0245
24	4	GI	2708	0.0111	0.0223	2249	0.0108	0.0216	0.831	0.0158	0.0312
24	5	GI	2713	0.0095	0.0189	2317	0.0137	0.0275	0.917	0.0161	0.0323
24	6	GI	2797	0.0090	0.0179	2333	0.0074	0.0149	0.824	0.0118	0.0233
24	7	GI	2974	0.0103	0.0206	2519	0.0109	0.0219	0.847	0.0148	0.0297
24	8	GI	2900	0.0102	0.0203	2462	0.0077	0.0153	0.849	0.0127	0.0255
24	9	GI	2753	0.0169	0.0337	2419	0.0135	0.0211	0.889	0.0169	0.0339
24	10	GI	2878	0.0111	0.0231	2396	0.0094	0.0188	0.832	0.0139	0.0277

Appendix C

TLD Data Results for TLDs Contained Within RANDO Phantom - StemRad Belt

Measurement Location			Belt Off				Belt On				Belt On / Belt Off		
Phantom Slice Number	Slice Cavity Number	Tissue Type	Absorbed Dose (mrad)	Relative Standard Uncertainty	Relative Expanded Uncertainty k=2		Absorbed Dose (mrad)	Relative Standard Uncertainty	Relative Expanded Uncertainty k=2		Ratio	Relative Standard Uncertainty	Relative Expanded Uncertainty k=2
24	11	GI	2866	0.0144	0.0288		2463	0.0114	0.0228		0.852	0.0184	0.0367
25	2	GI	2885	0.0147	0.0295		2164	0.0116	0.0233		0.747	0.0184	0.0368
25	3	GI	2762	0.0093	0.0187		2089	0.0113	0.0229		0.755	0.0146	0.0293
25	4	GI	2794	0.0158	0.0317		2077	0.0108	0.0216		0.766	0.0153	0.0306
25	5	GI	2755	0.0151	0.0303		2116	0.0163	0.0334		0.767	0.0229	0.0457
25	6	GI	2858	0.0091	0.0183		2132	0.0097	0.0193		0.746	0.0133	0.0266
25	7	GI	2990	0.0150	0.0300		2282	0.0117	0.0234		0.767	0.0194	0.0388
25	8	GI	2881	0.0097	0.0194		2287	0.0093	0.0186		0.794	0.0134	0.0269
25	9	GI	2883	0.0085	0.0169		2285	0.0141	0.0281		0.793	0.0164	0.0328
25	10	GI	2914	0.0087	0.0174		2294	0.0138	0.0276		0.787	0.0161	0.0321
25	11	GI	2987	0.0052	0.0104		2243	0.0164	0.0329		0.756	0.0301	0.0602
26	2	GI	2831	0.0082	0.0164		2055	0.0218	0.0435		0.726	0.0330	0.0660
26	3	GI	2767	0.0146	0.0291		1983	0.0189	0.0379		0.716	0.0239	0.0477
26	4	GI	2713	0.0124	0.0248		1953	0.0138	0.0277		0.720	0.0186	0.0372
26	5	GI	2721	0.0085	0.0170		1931	0.0161	0.0322		0.710	0.0132	0.0264
26	6	GI	2780	0.0076	0.0152		1936	0.0088	0.0176		0.696	0.0116	0.0232
26	7	GI	2589	0.0076	0.0153		2131	0.0100	0.0201		0.713	0.0126	0.0253
26	8	GI	2852	0.0093	0.0186		2110	0.0120	0.0239		0.702	0.0140	0.0280
26	9	GI	2820	0.0089	0.0178		2061	0.0079	0.0157		0.728	0.0117	0.0234
26	10	GI	2841	0.0079	0.0158		2037	0.0082	0.0165		0.717	0.0115	0.0229
26	11	GI	2837	0.0052	0.0103		2067	0.0087	0.0174		0.704	0.0119	0.0238
27	2	GI	2796	0.0125	0.0249		1932	0.0087	0.0174		0.678	0.0156	0.0315
27	3	GI	2751	0.0113	0.0229		1883	0.0164	0.0335		0.664	0.0215	0.0431
27	4	GI	2672	0.0102	0.0203		1852	0.0110	0.0219		0.667	0.0150	0.0299
27	5	GI	2657	0.0092	0.0183		1841	0.0121	0.0242		0.683	0.0150	0.0303
27	6	GI	2716	0.0079	0.0158		1829	0.0080	0.0160		0.673	0.0112	0.0226
27	7	GI	2934	0.0114	0.0227		1985	0.0135	0.0270		0.668	0.0177	0.0353
27	8	GI	2862	0.0130	0.0259		2016	0.0132	0.0264		0.704	0.0187	0.0374
27	9	GI	2820	0.0099	0.0198		1871	0.0086	0.0172		0.697	0.0131	0.0262
27	10	GI	2760	0.0136	0.0272		1915	0.0112	0.0224		0.687	0.0176	0.0352
27	11	GI	2953	0.0092	0.0184		1941	0.0080	0.0160		0.667	0.0122	0.0244
28	8	GI	2880	0.0101	0.0202		1798	0.0113	0.0227		0.623	0.0152	0.0304
28	9	GI	2761	0.0114	0.0228		1786	0.0078	0.0156		0.651	0.0138	0.0277
28	10	GI	2705	0.0094	0.0188		1767	0.0084	0.0167		0.653	0.0126	0.0252
28	11	GI	2741	0.0157	0.0315		1747	0.0180	0.0361		0.637	0.0238	0.0479
28	12	GI	2770	0.0206	0.0419		1729	0.0234	0.0469		0.624	0.0313	0.0626
28	13	GI	2879	0.0130	0.0264		1869	0.0094	0.0189		0.654	0.0163	0.0324
28	14	GI	2824	0.0094	0.0187		1890	0.0146	0.0292		0.669	0.0168	0.0337
28	15	GI	2951	0.0082	0.0165		1906	0.0120	0.0252		0.634	0.0151	0.0331
			min 2827	0.0076	0.0152	min	1726	0.0074	0.0148	min	0.62	0.0112	0.0224
			max 2990	0.0252	0.0504	max	2519	0.0234	0.0469	max	0.87	0.0313	0.0626
			average 2815	0.0110	0.0220	average	2051	0.0117	0.0233	average	0.74	0.0162	0.0324
			stdev 91	0.0035	0.0069	stdev	217	0.0037	0.0074	stdev	0.07	0.0045	0.0090
			%stdev 3.2			%stdev	10.6			%stdev	9.8		
32	6	ovary	2703	0.0091	0.0181		1767	0.0096	0.0191		0.653	0.0132	0.0264
33	7	ovary	2663	0.0104	0.0207		1767	0.0210	0.0419		0.664	0.0234	0.0469
			min 2663	0.0091	0.0181	min	1703	0.0096	0.0191	min	0.653	0.0132	0.0264
			max 2703	0.0104	0.0207	max	1767	0.0210	0.0419	max	0.659	0.0234	0.0469
			average 2683	0.0097	0.0194	average	1735	0.0153	0.0305	average	0.656	0.0183	0.0366
			stdev 14	0.0008	0.0016	stdev	2	0.0081	0.0161	stdev	0.00	0.0072	0.0144
			%stdev 0.5			%stdev	0.1			%stdev	0.7		

Note: RM7(and BM(x) are bone marrow in hip and vertebrae, respectively. GI is gastrointestinal tract, and OVARY are locations if this RANDO was female based on anatomical markers.

25	3	**	2987	0.0087	0.0174		2667	0.0099	0.0197		0.089	0.0131	0.0265

* The initial C.V. of the 3 chip readings for these measurement locations was larger than could be explained by the fundamental reproducibility of the TLD analysis system being used. The most possible explanation was that the stacking order of the chips within these 4 affected cavities was mixed up during the initial "Belt Off" irradiation and thus the chip identities and ECCs applied to the chips were mismatched. By properly re-matching ECCs to readings for each cavity, it was possible to obtain low C.V. values similar to the C.V. values for the unaffected locations. The same phantom loading sequence was used for both the "Belt Off" and the subsequent "Belt On" irradiations. The fact that the pattern of locations with large C.V. values was repeated in the second irradiation (Belt On) confirms that the stacking order was indeed mixed during the first irradiation. The fact that it was possible to re-match ECCs with chips to obtain low C.V. values in line with other locations, and the fact that the pattern of affected locations was repeated between first and second irradiations gives high confidence to our hypothesis that the stacking order of chips was mixed up during the first irradiation. The readings with initially applied ECCs, without ECCs, and with the correct ECCs applied are shown on the "Test Results (Belt Off)" and "Test Results (Belt On)" worksheets. The potential impact on the measured absorbed dose is also shown. The final values used for reporting purposes are based on the chip readings with properly matched ECCs. It should be noted that the mean absorbed dose value reported for each of the affected locations changed by less than 3% for all but one location as a result of the corrections made to the individual chip readings. The most affected location (Location 28-8 for "Belt On" irradiation), decreased by 8.4%, and the reported value is only 3.3% different than the equivalent cavity on the opposite side of phantom.

Appendix C

TLD Data Results for TLDs Contained Within RANDO Phantom - StemRad Belt

Measurement Location				Belt Off				Belt On				Belt On / Belt Off		
Phantom Slice Number	Slice Cavity Number	Tissue Type		Absorbed Dose (mrad)	Relative Standard Uncertainty	Relative Expanded Uncertainty k=2		Absorbed Dose (mrad)	Relative Standard Uncertainty	Relative Expanded Uncertainty k=2		Ratio	Relative Standard Uncertainty	Relative Expanded Uncertainty k=2
** This location in Slice # 13 was used as a quality control location to verify that equal doses were delivered at the phantom for the Belt Off and Belt On irradiations. The location was chosen such that it would not be influenced by the presence or absence of the shield belt.														

Background subtraction: For both rounds of phantom irradiations, the mean gross reading on unexposed blank chips was small compared to the gross reading of test chips exposed in phantom. The uncertainty in the mean gross reading of unexposed chips as represented by the standard error of the mean was negligible compared to the gross reading of even the lowest exposed test chips. Thus the uncertainty in the background reading was not included in the propagation of overall uncertainty for the measured absorbed doses reported above. Statistics on the gross readings of unexposed background control chips for each round of irradiations are shown below.

	Belt Off	Belt On
min (nC)	0.333	0.366
max (nC)	0.625	0.621
arithmetic mean (nC)	0.477	0.483
sample stdev (nC)	0.072	0.061
C.V.	0.150	0.041
n	51	51
std err of mean (nC)	0.010	0.009
std err of mean (mrad equivalent)	0.109	0.116

Reader Calibration: The uncertainty in calibration of the reader was calculated by combining the quoted fractional uncertainty (1 σ) in air kerma rates for the PNNL Cs-137 beam irradiator used to expose the TLD chips that were used to calibrate the Harshaw Model 6600 TLD reader (TTP 2) with the fractional uncertainty (1 σ) in reader response to the chips thusly exposed. The assessed fractional uncertainty in air kerma rate for this source (# 515-131) at the 3 meter distance is 0.0071. The fractional uncertainty in reader response was calculated from the relative standard error of the mean reader response in nanoCoulombs measured with 50 exposed TLD chips. The variability in reader response from chip to chip includes uncertainty in the assigned EDCs that are applied to the chip readings, as well as variability in reader sensitivity from readout to readout. The fractional uncertainty in reader response was determined to be 0.0023 for the belt off exposure condition and 0.0021 for the belt on exposure condition. Uncertainties in positioning during irradiation of calibration chips, and uncertainties in the conversion factor Ka used to convert from air kerma to Hp(10) were considered negligible and not included in the uncertainty calculation.

	Belt Off	Belt On
Delivered Dose (mrad)	1000	1000
Relative standard uncertainty in delivered dose	0.0071	0.0071
mean TL response (nC)	76.96	76.11
Relative standard uncertainty in TL response	0.0029	0.0021
Reader Calibration Factor - RCF (nC/mrad)	0.077	0.076
relative std uncertainty in RCF	0.00748	0.00748

Test Dosimeter Readings for each cavity: For each phantom measurement location, the fractional uncertainty in the TLD readout values was calculated as the standard error of the mean reading of the 3 chips in the chip cavity, divided by the mean. The 3 chip readings are considered to be repeated independent measurements of the same quantity. The mean is the unbiased estimate of the quantity and the standard error is an estimate of the uncertainty of the mean. The standard error of the mean for each cavity is calculated on the worksheets "Test Results (belt on)" and "Test Results (belt off).

Measured Absorbed Dose: For both the "belt on" and "belt off" test conditions, the Relative Standard Uncertainty (a.k.a. fractional uncertainty) in measured absorbed dose shown above for each measurement location, was calculated by combining the fractional uncertainty in mean test dosimeter reading for each cavity with the fractional uncertainty in reader calibration factor. This calculation is performed on the worksheets "Test Results (belt on)" and "Test Results (belt off)". The Relative Expanded Uncertainty was calculated from the relative standard uncertainty by multiplying by a coverage factor, k=2)

Absorbed Dose Ratio: For each measurement location shown above, the uncertainty in the reported ratio of absorbed dose with "Belt On" to the absorbed dose with "Belt Off" was calculated by combining the Relative Standard Uncertainty of the "Belt On" absorbed dose result with the Relative Standard Uncertainty of the "Belt Off" absorbed dose result.

Dosimetry-based Evaluation of StemRad Shielding Belt Effectiveness

Model Equation:

$Ratio_{b/o} = ((Dose_{belton} * Irrad_{offset}) / Dose_{beltoff})$;

$Dose_{belton} = TLDAvg_{belton}$;

$Dose_{beltoff} = TLDAvg_{beltoff}$;

$Irrad_{offset} = (distance_{belton}^2 / distance_{beltoff}^2) * S_{anisotropy} * S_{transit}$;

$distance_{belton} = 0.4*((h1+h_{op}+h_{os})^2+(l+l_{op}+l_{os})^2)^{0.5}+0.4*((h2+h_{op}+h_{os})^2+(l+l_{op}+l_{os})^2)^{0.5}+0.2*((h3+h_{op}+h_{os})^2+(l+l_{op}+l_{os})^2)^{0.5}$;

$distance_{beltoff} = 0.4*((h1)^2+(l)^2)^{0.5}+0.4*((h2)^2+(l)^2)^{0.5}+0.2*((h3)^2+(l)^2)^{0.5}$

List of Quantities:

Quantity	Unit	Definition
$Ratio_{b/o}$	unitless	Ratio of the Belt-on to Belt-off doses (shielding effectiveness)
$Dose_{belton}$	mrad	Dose determined from the irradiation with the shield belt on
$Irrad_{offset}$	unitless	Difference in
$Dose_{beltoff}$	mrad	Dose determined from the irradiation without the belt
$TLDAvg_{belton}$	mrad	Average of 3 chips irradiated with the belt on
$TLDAvg_{beltoff}$	mrad	Average of 3 chips irradiated with the belt off
$distance_{belton}$	cm	actual distance (incl. possible positioning errors)
$distance_{beltoff}$	cm	reference distance (composite of five levels)
$S_{anisotropy}$	unitless	Lateral anisotropy of the source (potential diffrence of the second irradiation versus the first)
$S_{transit}$	unitless	Influence of source placing the source and removing it from the irradiation position
h1	cm	(Height-1) Bottom and top offset distance from middle (reference) source height
h_{op}	cm	Height offset of phantom
h_{os}	cm	Height offset of source
l	cm	Lateral distance from source (at midpoint position)
l_{op}	cm	Lateral distance offset of phantom
l_{os}	cm	Lateral distance offset of source
h2	cm	(Height-2) Middle position between h1 and h2
h3	cm	(Height-3) Reference height - on the level of the phantom mid-point (Slice 29)

$TLDAvg_{beltoff}$: Type B trapezoid distribution
Value: 1.000 mrad
Halfwidth of Limits: 6.8 %
Shapefactor: 0.499

For the belt-on irradiation, the precision (2s) of the 3-chip readings ranged from 0.0148 to 0.0680. Only about 10 chip positions exceeded 0.0339. Therefore, will conclude this to be a trapezoidal distribution with Halfwidth of 6.80% and Shapefactor of 0.0339/0.0680, or 0.499.

$TLDAvg_{beltoff}$: Type B trapezoid distribution
Value: 1.000 mrad
Halfwidth of Limits: 5.04 %
Shapefactor: 0.595

For the baseline (reference) irradiation, the precision (2s) of the 3-chip readings ranged from 0.0152 to 0.0504. Only about 10 chip positions exceeded 0.0300. Therefore, will conclude this to be a trapezoidal distribution with Halfwidth of 5.04% and Shapefactor of 0.0300/0.0504, or 0.595.

$S_{anisotropy}$: Type B rectangular distribution
Value: 1.000 unitless
Halfwidth of Limits: 1 %

The source anisotropy has not been measured. 1% is a judgemental estimate; however, evidence from the reference TLDs placed at phantom slice 13 show the difference between the second and first irradiations to be within 1%. Based on that information, it is suspected that 1% is a conservatively high estimate.

$S_{transit}$: Type B rectangular distribution
Value: 1.000 unitless
Halfwidth of Limits: 0 unitless

Assume source was at 4' past the irradiation distance for about 10 sec. This will have negligible impact on the delivered dose to the phantom compared to the 8 hour irradiation time. Assign 0 influence for this.

h1: Constant
Value: 130 cm

This is the measured height of the source off the midline for the extreme elevations (lowest and highest). For the second (belt-on) irradiations, uncertainty of the measurement is assigned via source and phantom offset values, h_{os} and h_{op}, respectively.

h_{op}: Type B rectangular distribution
Value: 0 cm
Halfwidth of Limits: 0.3 cm

Estimated value by MKM

h_{os}: Type B rectangular distribution
Value: 0 cm
Halfwidth of Limits: 0.3 cm

Estimated value by MKM

l: Constant
Value: 130 cm

This is the measured lateral distance of the source to the reference point at slice 29 of the phantom. For the second (belt-on) irradiation, uncertainty of the measurement is assigned via source and phantom offset values, l_{os} and l_{op}, respectively.

l_{op}: Type B rectangular distribution
Value: 0 cm
Halfwidth of Limits: 0.3 cm

Estimated value by MKM

l_{os}: Type B rectangular distribution
Value: 0 cm
Halfwidth of Limits: 0.3 cm

Estimated value by MKM

h2: Constant
Value: 54 cm

This is the measured height of the source off the midline for the mid elevations (middle lower and middle upper). For the second (belt-on) irradiations, uncertainty of the measurement is assigned via source and phantom offset values, h_{os} and h_{op}, respectively.

h3: Constant
Value: 0 cm

This is the measured height of the source at the midline. For the second (belt-on) irradiations, uncertainty of the measurement is assigned via source and phantom offset values, h_{os} and h_{op}, respectively.

Uncertainty Budgets:

$Ratio_{abs}$: Ratio of the Belt-on to Belt-off doses (shielding effectiveness)

Quantity	Value	Standard Uncertainty	Distribution	Sensitivity Coefficient	Uncertainty Contribution	Index
$TLDAvg_{belton}$	1.0000 mrad	0.0310 mrad	trapezoidal	1.0	0.031 unitless	61.0 %
$TLDAvg_{beltoff}$	1.0000 mrad	0.0239 mrad	trapezoidal	-1.0	-0.024 unitless	36.3 %
$S_{anisotropy}$	1.00000 unitless	0.00577 unitless	rectangular	1.0	$5.8 \cdot 10^{-3}$ unitless	2.1 %
$S_{transit}$	1.0 unitless	0.0 unitless	rectangular	0.0	0.0 unitless	0.0 %
h1	130.0 cm					
h_{up}	0.0 cm	0.173 cm	rectangular	$5.6 \cdot 10^{-3}$	$970 \cdot 10^{-6}$ unitless	0.0 %
h_{low}	0.0 cm	0.173 cm	rectangular	$5.6 \cdot 10^{-3}$	$970 \cdot 10^{-6}$ unitless	0.0 %
l	130.0 cm					
l_{up}	0.0 cm	0.173 cm	rectangular	0.011	$1.9 \cdot 10^{-3}$ unitless	0.2 %
l_{low}	0.0 cm	0.173 cm	rectangular	0.011	$1.9 \cdot 10^{-3}$ unitless	0.2 %
h2	54.0 cm					
h3	0.0 cm					
$Ratio_{abs}$	1.0000 unitless	0.0387 unitless				

$Dose_{belton}$: Dose determined from the irradiation with the shield belt on

Quantity	Value	Standard Uncertainty	Distribution	Sensitivity Coefficient	Uncertainty Contribution	Index
$TLDAvg_{belton}$	1.0000 mrad	0.0310 mrad	trapezoidal	1.0	0.031 mrad	100.0 %
$Dose_{belton}$	1.0000 mrad	0.0310 mrad				

$Irrad_{offset}$: **Difference in**

Quantity	Value	Standard Uncertainty	Distribution	Sensitivity Coefficient	Uncertainty Contribution	Index
$S_{anisotropy}$	1.00000 unitless	0.00577 unitless	rectangular	1.0	$5.8 \cdot 10^{-3}$ unitless	78.6 %
S_{stemrd}	1.0 unitless	0.0 unitless	rectangular	0.0	0.0 unitless	0.0 %
h1	130.0 cm					
h_{up}	0.0 cm	0.173 cm	rectangular	$5.6 \cdot 10^{-3}$	$970 \cdot 10^{-6}$ unitless	2.2 %
h_{bo}	0.0 cm	0.173 cm	rectangular	$5.6 \cdot 10^{-3}$	$970 \cdot 10^{-6}$ unitless	2.2 %
l	130.0 cm					
l_{up}	0.0 cm	0.173 cm	rectangular	0.011	$1.9 \cdot 10^{-3}$ unitless	8.5 %
l_{ao}	0.0 cm	0.173 cm	rectangular	0.011	$1.9 \cdot 10^{-3}$ unitless	8.5 %
h2	54.0 cm					
h3	0.0 cm					
$Irrad_{offset}$	1.00000 unitless	0.00651 unitless				

$Dose_{belton}$: **Dose determined from the irradiation without the belt**

Quantity	Value	Standard Uncertainty	Distribution	Sensitivity Coefficient	Uncertainty Contribution	Index
$TLDAvg_{beltoff}$	1.0000 mrad	0.0239 mrad	trapezoidal	1.0	0.024 mrad	100.0 %
$Dose_{beltoff}$	1.0000 mrad	0.0239 mrad				

$distance_{belton}$: **actual distance (incl. possible positioning errors)**

Quantity	Value	Standard Uncertainty	Distribution	Sensitivity Coefficient	Uncertainty Contribution	Index
h1	130.0 cm					
h_{up}	0.0 cm	0.173 cm	rectangular	0.44	0.076 cm	10.4 %
h_{bo}	0.0 cm	0.173 cm	rectangular	0.44	0.076 cm	10.4 %
l	130.0 cm					
l_{up}	0.0 cm	0.173 cm	rectangular	0.85	0.15 cm	39.6 %
l_{ao}	0.0 cm	0.173 cm	rectangular	0.85	0.15 cm	39.6 %
h2	54.0 cm					
h3	0.0 cm					
distance belton	155.847 cm	0.235 cm				

This distance is assigned uncertainty based on how well the positioning of the second (belt-on) irradiation configuration replicates the reference conditions (belt-off). Values for h1, h2, h3 and l are considered as constants for convenience, but each is then assigned offset influences associated with lateral distance and height of both the source and the phantom. The distance for the irradiation is taken to be a weighted composite of all of the five distances, consisting of two heights below the source midpoint and two hieghts above. The distance from the source to the phantom reference point (center of the phantom of slice 29) is calculated as the hypoteneuse of the various angles formed by heights (h1, h2 and h3) and lateral distance (l). Since there are five equal dose intervals, 40% of the dose comes from height h1, 40% from height h2 and 20% from height h3.

$distance_{beltoff}$: reference distance (composite of five levels)

Quantity	Value	Standard Uncertainty	Distribution	Sensitivity Coefficient	Uncertainty Contribution	Index
h1	130.0 cm					
l	130.0 cm					
h2	64.0 cm					
h3	0.0 cm					
distance beltoff	155.84683117866 cm	0.0 cm				

This distance is assumed to be the reference distance. Since this is a comparative assessment (i.e., relative evaluation), the irradiation with the belt off is assume to be performed at an absolute distance. Therefore, values for h1, h2, h3 and l are considered to be constants. The distance for the irradiation is taken to be a weighted composite of all of the five distances, consisting of two heights below the source midpoint and two hieghts above. The distance from the source to the phantom reference point (center of the phantom of slice 29) is calculated as the hypoteneuse of the various angles formed by heights (h1, h2 and h3) and lateral distance (l). Since there are five equal dose intervals, 40% of the dose comes from height h1, 40% from height h2 and 20% from height h3.

Results:

Quantity	Value	Expanded Uncertainty	Coverage factor	Coverage
$Ratio_{ccc}$	1.000 unitless	7.9 % (relative)	2.00	95% (normal)
$Dose_{beltoff}$	1.000 mrad	6.2 % (relative)	2.00	95% (normal)
$Irrad_{offset}$	1.000 unitless	1.3 % (relative)	2.00	95% (normal)
$Dose_{beltoff}$	1.000 mrad	4.8 % (relative)	2.00	95% (normal)
$distance_{beltoff}$	155.85 cm	0.30 % (relative)	2.00	95% (normal)
$distance_{beltoff}$	155.84683117866 cm	0.0 % (relative)	2.00	95% (normal)